REPORT SSD-TR-89-85

(4)

AD-A215 763

Observation of the Rabi-Resonance Spectrum

Prepared by

J. C. CAMPARO and R. P. FRUEHOLZ
Chemistry and Physics Laboratory
The Aerospace Corporation
El Segundo, CA 90245

30 September 1989

Prepared for

SPACE SYSTEMS DIVISION
AIR FORCE SYSTEMS COMMAND
Los Angeles Air Force Base
P.O. Box 92960
Los Angeles, CA 90009-2960

89 12

This report was submitted by The Aerospace Corporation, El Segundo, CA 90245, under Contract No. F04701-85-C-0086-P00016 with the Space Division, P.O. Box 92960, Los Angeles, CA 90009-2960. It was reviewed and approved for The Aerospace Corporation by S. Feuerstein, Director, Chemistry and Physics Laboratory.

Capt Michael Mitchell was the project officer for the Mission-Oriented Investigation and Experimentation (MOIE) Program.

This report has been reviewed by the Public Affairs Office (PAS) and is releasable to the National Technical Information Service (NTIS). At NTIS, it will be available to the general public, including foreign nationals.

This technical report has been reviewed and is approved for publication. Publication of this report does not constitute Air Force approval of the report's findings or conclusions. It is published only for the exchange and stimulation of ideas.

Michael J. Mitchell

MICHAEL MITCHELL, CAPT, USAF
MOIE Project Officer
SSD/CWNZ

Raymond M Leong

RAYMOND LEONG, MAJ, USAF
MOIE Program Manager
AFSTC/WCO OL-AB

UNCLASSIFIED

SECURITY CLASSIFICATION OF THIS PAGE

REPORT DOCUMENTATION PAGE

1a. REPORT SECURITY CLASSIFICATION Unclassified	1b. RESTRICTIVE MARKINGS
2a. SECURITY CLASSIFICATION AUTHORITY	3. DISTRIBUTION/AVAILABILITY OF REPORT Approved for public release; distribution unlimited.
2b. DECLASSIFICATION/DOWNGRADING SCHEDULE	
4. PERFORMING ORGANIZATION REPORT NUMBER(S) TR-0089(4945-05)-2	5. MONITORING ORGANIZATION REPORT NUMBER(S) SSD-TR-89-85
6a. NAME OF PERFORMING ORGANIZATION The Aerospace Corporation Laboratory Operations 6b. OFFICE SYMBOL (If applicable)	7a. NAME OF MONITORING ORGANIZATION Space Systems Division
6c. ADDRESS (City, State, and ZIP Code) El Segundo, CA 90245	7b. ADDRESS (City, State, and ZIP Code) Los Angeles Air Force Base Los Angeles, CA 90009-2960
8a. NAME OF FUNDING/SPONSORING ORGANIZATION 8b. OFFICE SYMBOL (If applicable)	9. PROCUREMENT INSTRUMENT IDENTIFICATION NUMBER F04701-88-C-0089
8c. ADDRESS (City, State, and ZIP Code)	10. SOURCE OF FUNDING NUMBERS PROGRAM ELEMENT NO. / PROJECT NO. / TASK NO / WORK UNIT ACCESSION NO

11. TITLE (Include Security Classification)

Observation of the Rabi-Resonance Spectrum

12. PERSONAL AUTHOR(S)

Camparo, James C. and Frueholz, Robert P.

13a. TYPE OF REPORT	13b. TIME COVERED	14. DATE OF REPORT (Year, Month, Day)	15. PAGE COUNT
	FROM _____ TO _____	1989 September 30	30

16. SUPPLEMENTARY NOTATION

17. COSATI CODES			18. SUBJECT TERMS (Continue on reverse if necessary and identify by block number)
FIELD	GROUP	SUB-GROUP	Coherent Processes Transient Phenomena

19. ABSTRACT (Continue on reverse if necessary and identify by block number)

By use of a double-resonance technique, a spectrum of Rabi resonances has been observed. These resonances are enhancements in the dynamic response of a quantum system's population to rapid changes in the phase of a perturbing electromagnetic field. Theoretically, it is shown that the appearance of a spectrum, as opposed to a single Rabi resonance, is due to the fact that the phase of the field changes discretely by π radians, rather than sinusoidally. In the presence of π-radian phase changes, the quantum system's dynamic response is found to be similar to a damped harmonic oscillator driven by a delta function force term. In this harmonic-oscillator approximation the Rabi-resonance spectrum arises naturally, resulting from a resonant enhancement of the atomic coherence.

20. DISTRIBUTION/AVAILABILITY OF ABSTRACT	21. ABSTRACT SECURITY CLASSIFICATION	
☒ UNCLASSIFIED/UNLIMITED ☐ SAME AS RPT ☐ DTIC USERS	Unclassified	
22a. NAME OF RESPONSIBLE INDIVIDUAL	22b. TELEPHONE (Include Area Code)	22c. OFFICE SYMBOL

DD FORM 1473, 84 MAR

83 APR edition may be used until exhausted
All other editions are obsolete

SECURITY CLASSIFICATION OF THIS PAGE

UNCLASSIFIED

PREFACE

We wish to thank P. Lambropoulous for several stimulating and enlightening discussions regarding the effects of rapid field phase changes on quantum systems.

CONTENTS

FIGURES

I. INTRODUCTION

It is well known that when a quantum system is interacting strongly with resonant electromagnetic radiation, a rapid change in the amplitude or wavelength of the radiation field will induce a transient response in the quantum system's wave function.[1] However, the dynamic response of a quantum system to rapid field phase changes is not well understood, and recently there has been an increasing interest in this question. For example, Helisto et al.,[2] Ikonen et al.[3] and Realo et al.,[4,5] investigating the consequences of rapid field phase changes in Mossbauer spectroscopy, have found that short bursts of gamma ray photons are generated when a resonant absorber is placed in the path of a "phase-switched" gamma-ray field. In the optical regime several groups have initiated detailed studies of various coherent transients resulting from laser-field phase switching.[6-10] Of particular note is the work of Bai et al.,[11] where Yb atoms were prepared in specific dressed states. Taken together, these individual results indicate the breadth of phenomena associated with rapid electromagnatic field phase changes, and the new information to be gained concerning the resonant interaction of radiation and matter.

Of considerable significance in this regard is the work of Cappeller and Mueller, and their observation of so called "Rabi resonances."[12] A Rabi-resonance is an enhancement in the transient response of a quantum system to a train of radiation-field phase changes (in the case of Cappeller and Mueller this was observed as an increase in the amplitude of quantum system population oscillations), when the rate of phase changing satisfies a resonance-like condition with the Rabi frequency. Whereas Cappeller and Mueller[12] varied the phase of their strong field smoothly (sinusoidally), and observed only a single Rabi resonance for a given radiation-field amplitude; in the present work we vary the field discretely and find a Rabi-resonance spectrum. In the following sections of this report it will be shown that the spectrum is a consequence of the discrete nature of the phase change, and that it may be easily understood in the framework of a harmonic oscillator driven by a periodic delta-function force.

II. EXPERIMENT

The experimental arrangement and atomic energy levels of interest are shown in Figure 1. A Corning 7070 glass cell containing 10 torr of nitrogen and a saturated vapor of Rb^{87} was contained within a microwave cavity whose TE_{011} mode resonated at roughly 6835 MHz. The cell length was 7 cm, and the pool of liquid Rb was maintained at a constant temperature; typically the cell temperatures ranged from 30 to 50°C. The microwave cavity and cell were placed in a large solenoid, which provided a static magnetic field of hundreds of milligauss in the direction of the oscillating microwave magnetic field; the static field removed the degeneracy of the hyperfine manifolds, and ensured that the microwave field was only resonant with the ground state (m_F=0) - (m_F=0) hyperfine transition. The microwave field was the strong field in these experiments, and saturated the 0-0 transition. By observing the transmitted light of a diode laser whose frequency was resonant with the D_2, $5^2P_{3/2}$ - $5^2S_{1/2}$, transition at 780.2 nm, the population in one of the hyperfine manifolds was monitored. The transmitted light was detected with a silicon photodiode and amplified, and the transients were averaged with a Nicolet 1140 Signal Averager. The bandwidth of the measurement system was roughly 300 kHz, much faster than any dynamic rate in the quantum system.

In order to create a population imbalance between the two hyperfine levels coupled by the microwave field, the diode laser was employed for optical pumping[13,14] as well as detection. The diode laser, with a linewidth of 70 MHz and an output power of 1.8 mW, selectively excited atoms out of the F=2 hyperfine manifold. The Doppler broadened linewidth of the Rb^{87} D_2 transition at 30°C is 514 MHz, which allowed resolution of the ground state, but not excited state, hyperfine splitting. Since atoms in the $5^2P_{3/2}$ state can return to either of the ground-state hyperfine manifolds, the consequence of several absorption and emission cycles was the reduction of population in the F=2 hyperfine manifold. Once an optical pumping equilibrium had been attained, the transmitted diode laser

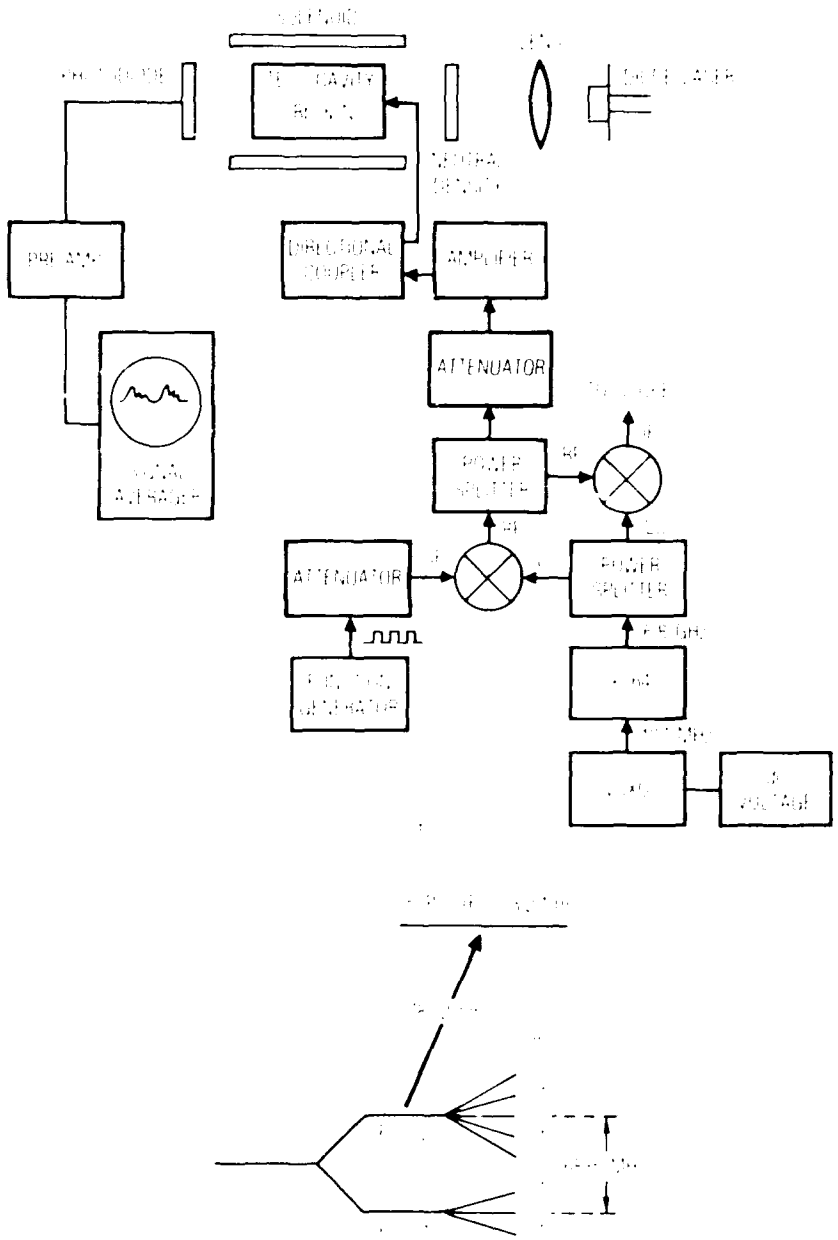

Figure 1. (a) Experimental arrangement used in the present study, and described in the text. (b) Atoms optically pumped out of the F=2 ground-state hyperfine manifold by the 780.2-nm diode laser light; the transmission of this laser light also serves to monitor the population in the F=2 manifold. A static magnetic field splits the ground-state Zeeman sublevels, so that the 6835-MHz microwaves only couple the m_F=0 states.

intensity was at a maximum. When the vapor was then exposed to the resonant microwave field, atoms returned to the F=2 hyperfine manifold, and the transmitted light intensity decreased. The level of transmitted light intensity was used as a measure of the population density in the F=2 hyperfine manifold, and transient effects in the population density were easily observed when the phase of the microwave field changed rapidly.

A voltage-controlled crystal oscillator (VCXO) with a nominal frequency of 107 MHz was the starting point for the generation of a phase-switched microwave field. The VCXO output was multiplied to 6835 MHz and split into two paths. One path went to the phase-switching mixer, and the other went to the phase-detecting mixer. In the phase-switching mixer the microwave signal was combined with a square wave, so that the output of the mixer was a 6835-MHz signal whose phase jumped discretely by π radians at a rate twice the square wave frequency. This phase-switched field was again split into two paths, one path leading to the microwave cavity and the experiment, and the other path leading to the phase-detecting mixer. In the phase-detecting mixer, the phase-switched field was combined with the original microwave field to produce an output signal whose voltage was proportional to the phase difference between the two inputs. This signal was then used to observe the phase changes, and to ensure that the rise time for the phase change was much faster than any dynamic rate in the quantum system. In the experiments of the present work the microwaves were always resonant with the 0-0 hyperfine transition frequency.

The above experimental design has several characteristics that make the arrangement well suited to the study of population transients following rapid field phase changes:

1. The ground state 0-0 hyperfine transition is a good approximation to a two-level quantum system.

2. Atomic dephasing and longitudinal relaxation can be manipulated experimentally by simply adjusting the optical pumping rate.[13,15]

3. Inhomogeneous Doppler broadening is removed by the Dicke mechanism of motional narrowing.[16,17]

III. RESULTS

Figure 2(a) shows an example of the experimental transmitted light intensity oscillations that were observed when the phase of the strong microwave field changed by π radians. Immediately following the abrupt phase change there is an initial increase in the transmitted light intensity, which corresponds to an initial decrease in the atomic population density in the optically absorbing hyperfine manifold. The quantum system tends towards its unsaturated state (i.e., its state in the absence of the saturating microwave field). This initial increase is subsequently followed by a decrease in the transmitted light intensity, yielding an eventual pattern of damped transmitted light intensity oscillations. In the Appendix it is shown that the amplitudes of the transmitted light intensity oscillations are proportional to the amplitudes of the corresponding population oscillations; thus, the light intensity oscillations of Figure 2(a) imply a gross, coherent movement of atomic population between the two hyperfine manifolds. As will be discussed in Section IV, these effects are predicted by both a two-level and nondegenerate multilevel numerical density-matrix calculation of the transient effects. The figure also shows that the oscillations following the first full oscillation were sitting on some dying exponential; this is not predicted by either set of density-matrix calculations, and at the present time is not fully understood. This latter effect does not significantly impact the results to be reported here, as our attention is restricted to the relative amplitude of the population oscillations. Figure 2(b) shows the response of the atomic population to a train of phase changes with the phase-changing rate selected to yield maximum population oscillations. Note the cusp-like shape of the lower portion of the oscillations; the origin of this shape will be discussed subsequently.

The amplitude of the first population oscillation after a phase change exhibits a marked sensitivity to the microwave Rabi frequency as shown in Figure 3. The two sets of experimental data correspond to two different

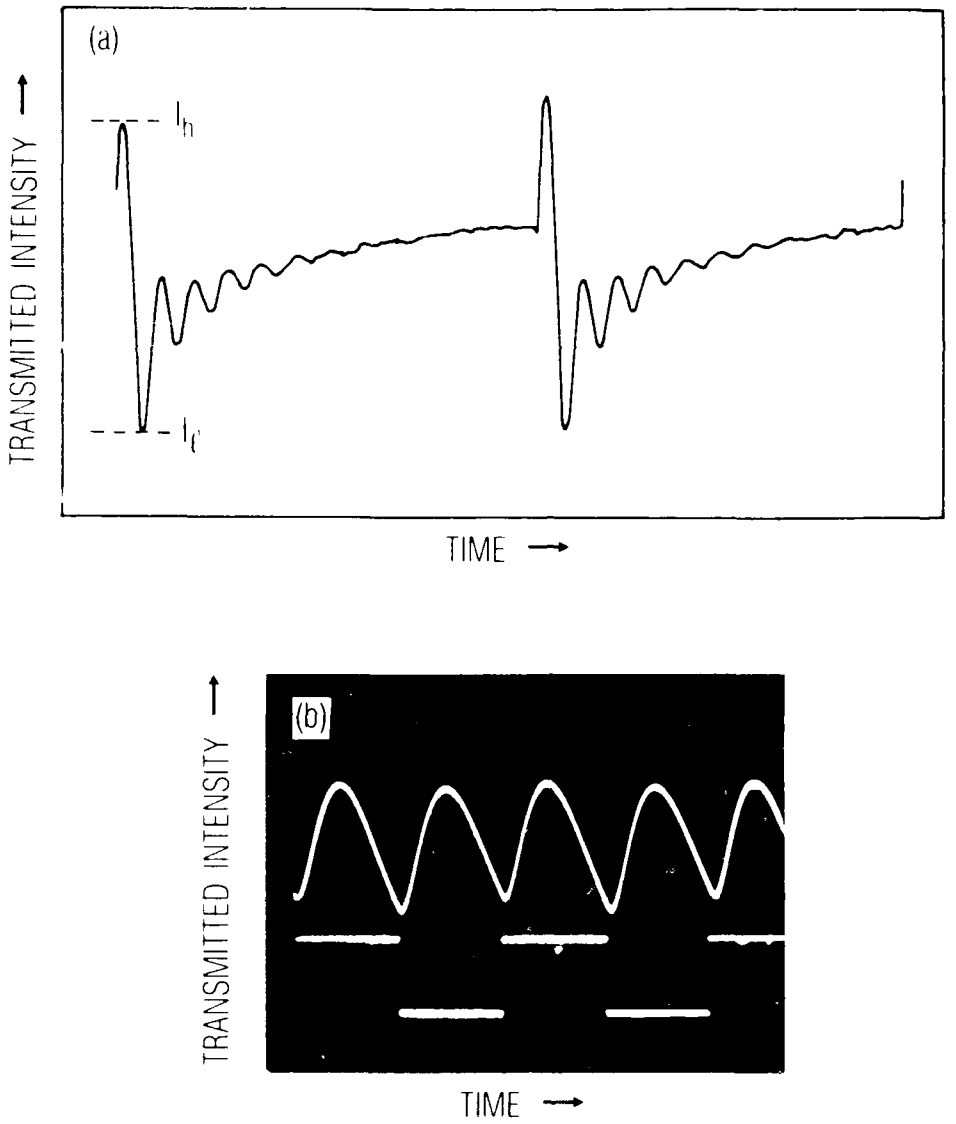

Figure 2. (a) Following a change in the phase of the microwave field by π radians, the transmitted diode laser light intensity shows decaying oscillatory behavior. In the limit of low optical pumping rates or optically thin vapors, the transmitted intensity oscillations are proportional to changes in the population of the optically absorbing state. For the experiment which led to the above oscillations the temperature of the resonance cell was approximately 33°C and a neutral density of 2.3 was placed in the laser beam path. (b) Response of the atomic population to a train of π radian phase changes, with the phase changing rate selected to yield maximum population oscillations. The upper trace shows the transmitted intensity variation, whereas the lower trace shows the output from the phase-detection mixer. Note the cusp-like appearance of the transmitted intensity oscillations.

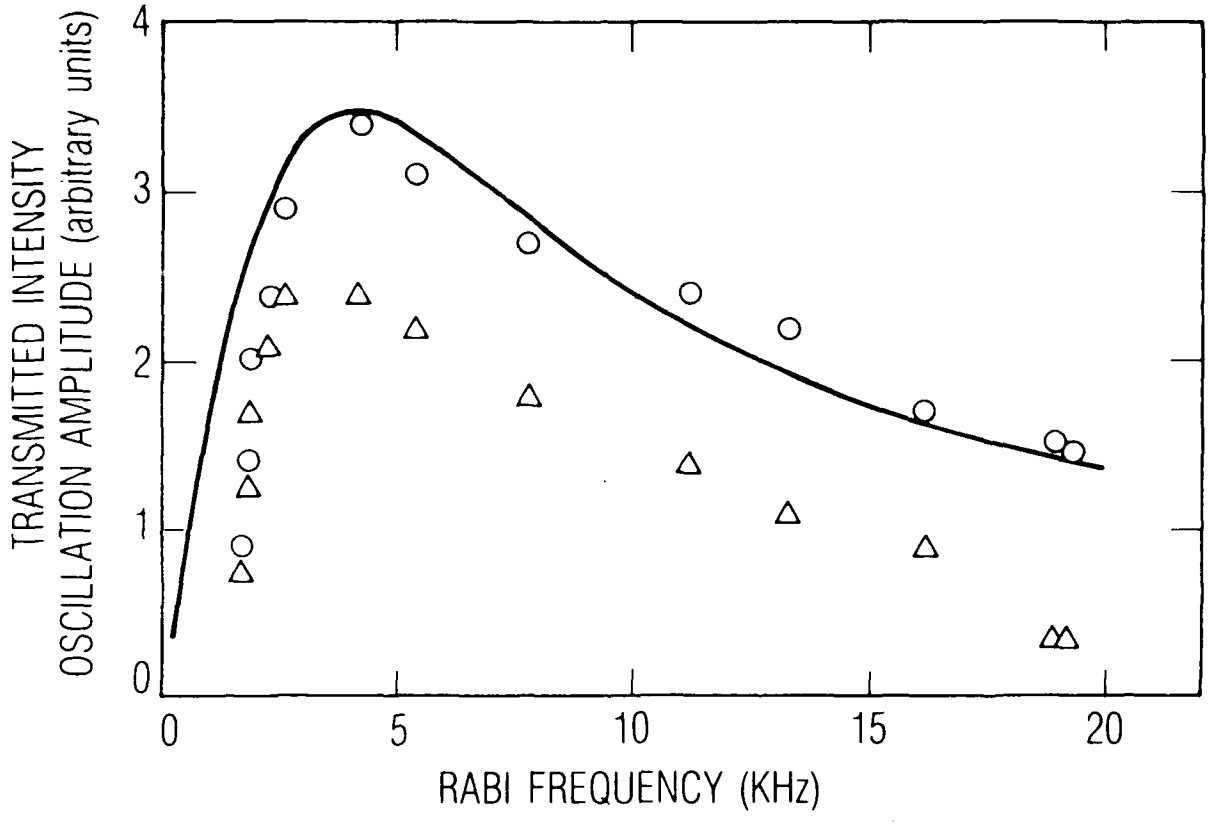

Figure 3. Amplitude of the first oscillation following a phase change is a sensitive function of the Rabi frequency. Triangles correspond to phase-changing rates where the quantum system had time to reach equilibrium before the next phase change occurred; open circles correspond to a phase-changing rate that satisfied the Rabi-resonance condition as discussed in the text. The solid line is the theoretical steady-state coherence, which is given by Eq. (8), suitably normalized and with $\Gamma = \Gamma_1 = \Gamma_2$ chosen to give a maximum at the appropriate Rabi frequency. For this experiment the resonance cell temperature was approximately 50°C and a neutral density filter of 1.0 was in the laser beam-path.

values of the phase-changing rate. In the first data set the rate of phase changing was very low, so that the quantum system reached equilibrium in the time between successive phase changes. In the second data set the rate of phase changing was chosen so as to satisfy a Rabi-resonance condition leading to enhanced population oscillations. For both experimental situations it is clear that there was an optimum Rabi frequency for producing large population oscillations, and that the value of this optimum Rabi frequency was relatively insensitive to the rate of phase changing.

In Figure 4 we show the Rabi-resonance profile that was obtained in the present experiment. Here, the amplitude of the first transmitted intensity oscillation following a phase change was measured as a function of the rate of phase changing, and it is clear that a "spectrum" of Rabi resonances was found. The observation of a Rabi-resonance spectrum is in marked contrast to the results of Cappeller and Mueller,[12] where only a single Rabi resonance was obtained. For phase-changing rates much higher than the Rabi frequency (which in these experiments was roughly a kilohertz) the amplitude of the population oscillations approaches zero asymptotically. In Section IV these results will be discussed within a harmonic-oscillator approximation of the coherent phenomenon.

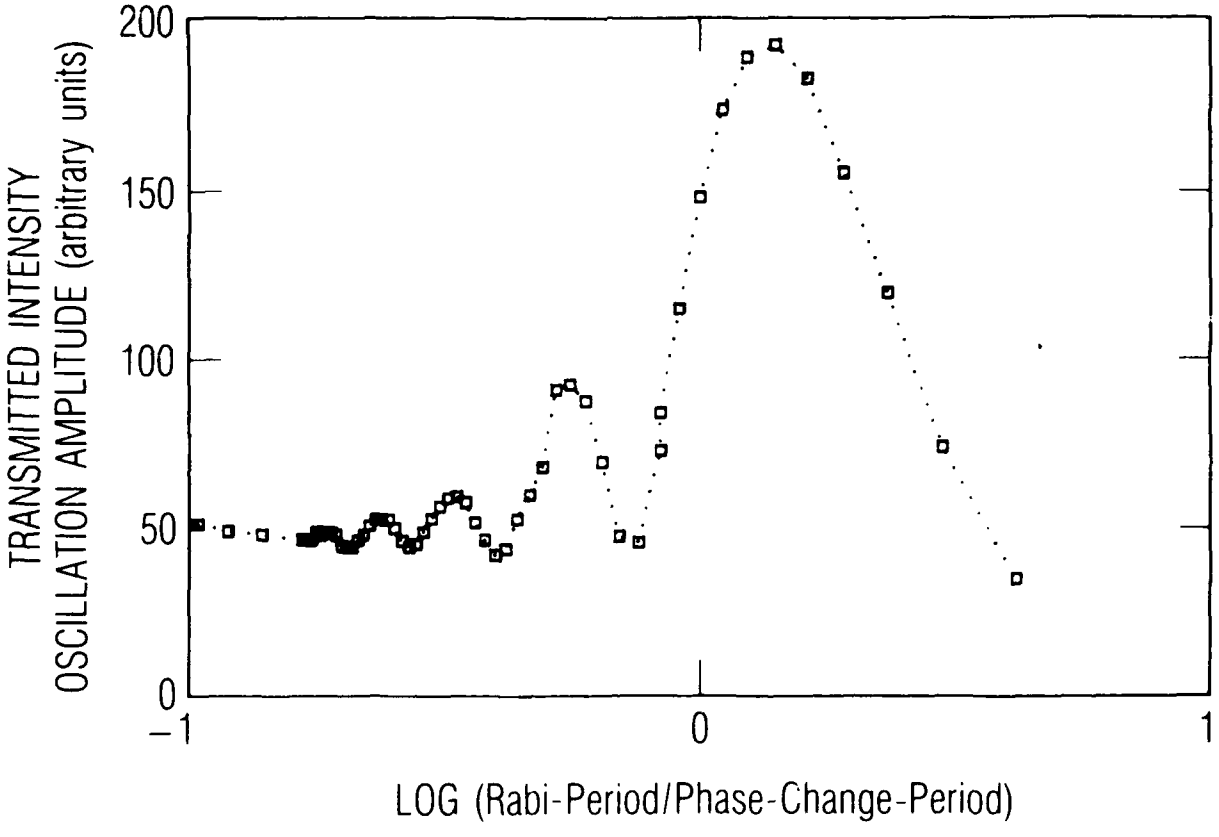

Figure 4. When examined as a function of the phase-changing rate the amplitude of the population oscillations shows resonant behavior producing a Rabi-resonance spectrum. The Rabi frequency was determined by measuring the temporal duration of the first oscillation. Experimental points are indicated by squares; dots between data points are simply an aid to guide the eye.

IV. ANALYSIS

A. NUMERICAL ANALYSIS

To verify that the physical mechanisms leading to the observed phenomena are understood on a formal level, one can consider numerical solutions of the density-matrix equations describing the experimental system with optical pumping. In this regard the quantum system is approximated as a two-level atom, since the field only interacts with the $m_F = 0$ states:

$$\dot{\sigma}_{11} = -\Gamma_1 \sigma_{11} + \Omega \sin[\theta(t)]\, \mathrm{Im}(\sigma_{12}) + \Omega \cos[\theta(t)]\, \mathrm{Re}(\sigma_{12}) + 0.5\,(\gamma_1 + B), \tag{1a}$$

$$\mathrm{Re}(\dot{\sigma}_{12}) = -\Gamma_2\, \mathrm{Re}(\sigma_{12}) + \frac{\Omega}{2} \cos[\theta(t)]\,(1-2\sigma_{11}), \tag{1b}$$

$$\mathrm{Im}(\dot{\sigma}_{12}) = -\Gamma_2 \mathrm{Im}(\sigma_{12}) + \Omega\, \sigma_{11} \sin[\theta(t)] - \frac{\Omega}{2} \sin[\theta(t)], \tag{1c}$$

with $\Gamma_i = (\gamma_i + B/2)$. Here, σ_{11} is the density matrix element describing the population in the lower energy state of the quantum system, σ_{12} is the coherence term of the density matrix, γ_1 and γ_2 are, respectively, the longitudinal and transverse (dephasing) relaxation rates, B is the optical photon absorption rate, Ω is the hyperfine transition Rabi frequency, and $\theta(t)$ is the phase angle of the strong field at the time t.

Numerical solutions for the transient response of the lower level's population (actually $\sigma_{11} - \sigma^{ss}$, where σ^{ss} is the steady state value) and the real part of the system's coherence ($\mathrm{Re}(\sigma_{12})$) are displayed in Figure 5. These results are essentially the same as those produced by an eight-level density matrix analysis,[18] rigorously correct for the ground state of Rb^{87}. The similarity of the solutions is due to the fact that on the time scales of interest the various Zeeman sublevels are not strongly coupled.[19] Note that the results do not predict an exponential decay in

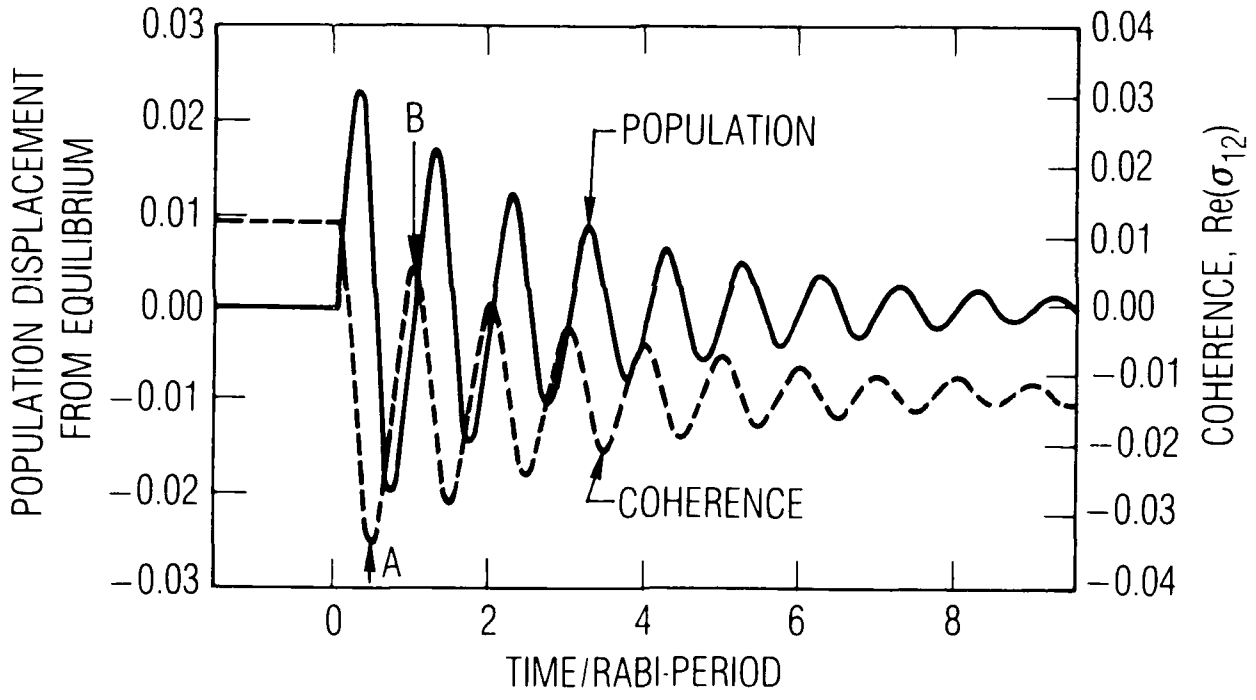

Figure 5. Theoretical oscillations of the quantum system's population ($\sigma_{11} - \sigma^{ss}$) and the real part of its coherence following a π-radian phase change for a two-level atom. Results were computed by numerically solving Eqs. (1a) to (1c), and are plotted as functions of time normalized to the Rabi period. For this calculation $\gamma_1/\Omega = \gamma_2/\Omega = 0.025$ and $B/\Omega = 0.05$. Points A and B are discussed in the text.

the transient response as was observed in the experiment. Consequently, it may be inferred that the experimental decay is not a simple consequence of phase switching in either a two- or eight-level quantum system. However, as evidenced by the similarity between Figure (6a), which shows the two-level density-matrix prediction of the Rabi resonance spectrum, and Figure 4, the presence of the exponential has relatively little impact on the spectrum's appearance.

Comparing the theoretical Rabi-resonance spectrum with the experimental spectrum, it is clear that the numerical two-level density-matrix calculations do well in predicting the quantum system's observed behavior: (a) the four largest resonances occur within a decade change of the Rabi frequency, (b) the amplitude of the resonances is an increasing function of Rabi frequency, and (c) for phase changing rates higher than roughly twice the Rabi frequency, the quantum system response asymptotically approaches zero. However, if in the calculations we allow the phase angle in Eqs. (1a) to (1c) to vary sinusoidally, rather than discretely, then the Rabi resonance spectrum collapses to a single resonance as shown in Figure 6(b). This result indicates that it is the discrete π-radian nature of the phase change that leads to the appearance of a Rabi-resonance spectrum. Unfortunately, the interplay between the discrete phase changes and the quantum system's response that results in the Rabi-resonance spectrum is not elucidated by the numerical results; consequently, in Section IVB we consider an approximate, but analytic, solution to the equations describing the quantum system's dynamic behavior.

B. ANALYTIC SOLUTION

To develop the desired physical insight we first note that the response of the atomic population to a single phase change (Figures 2 and 5) is suggestive of the response of a damped harmonic oscillator, when it is subjected to an impulse excitation. Similarly, the Rabi-resonance spectrum brings to mind the response of a sequentially excited harmonic system. This leads us to investigate a "harmonic approximation" to the atomic density-matrix equations.

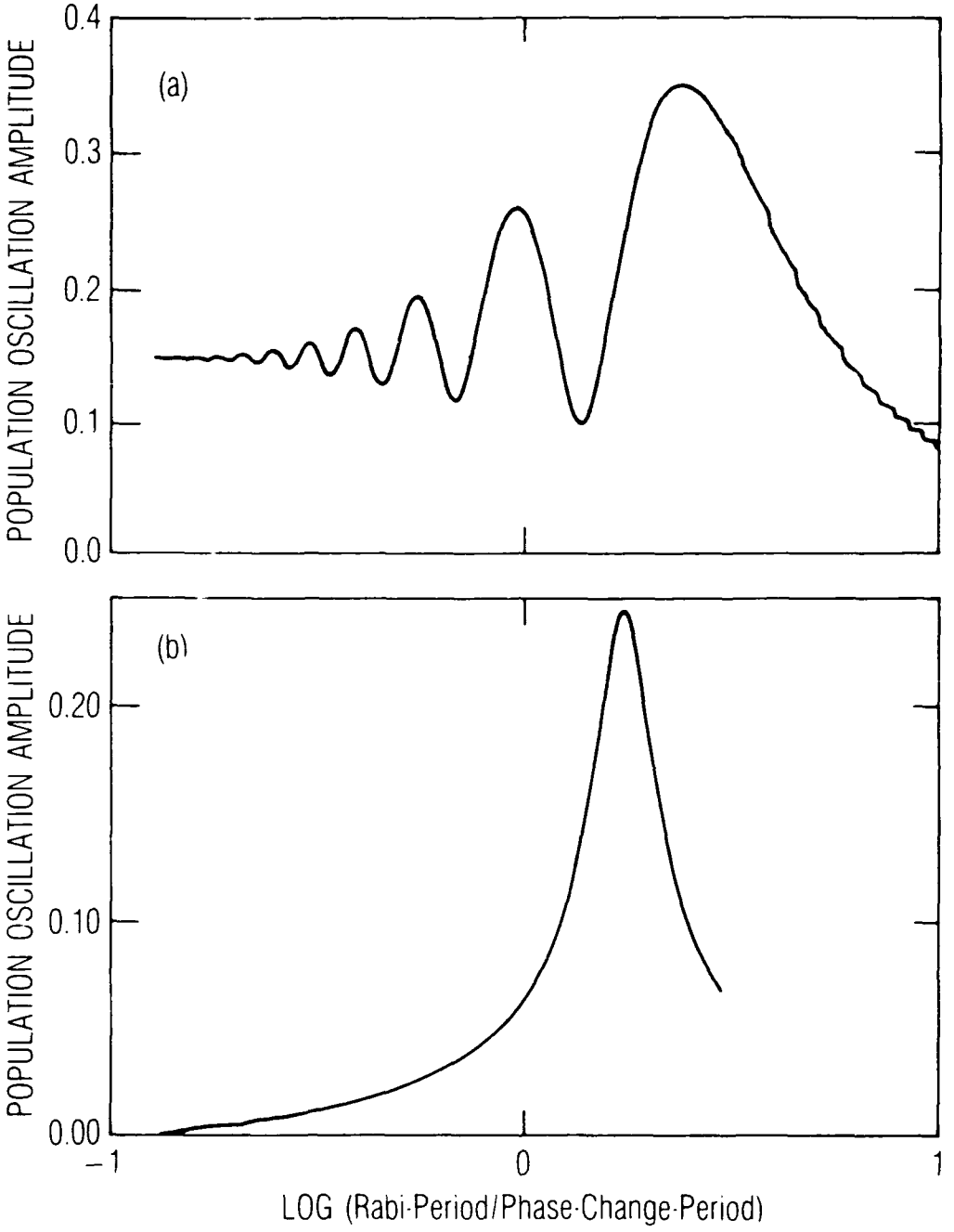

Figure 6. (a) Numerical solutions to the two-level atom density matrix equations showing the predicted Rabi-resonance spectrum. As discussed in the text the appearance of this spectrum is in good agreement with experimental observations. (b) Same calculation as in (a) except that the phase is allowed to vary sinusoidally between 0 and 2π radians at the phase-changing frequency.

When $\theta(t)$ changes discretely from 0 to π and vice versa, Eqs. (1a to 1c) take the form

$$\dot{\sigma}_{11} = - \Gamma_1 \sigma_{11} + \Omega h \, \mathrm{Re}(\sigma_{12}) + 0.5 \, (\gamma_1 + B) \tag{2a}$$

$$\mathrm{Re}(\dot{\sigma}_{12}) = - \Gamma_2 \, \mathrm{Re}(\sigma_{12}) - 0.5 \, \Omega \, h \, (1-2\sigma_{11}) \tag{2b}$$

$$\mathrm{Im}(\dot{\sigma}_{12}) = - \Gamma_2 \, \mathrm{Im}(\sigma_{12}), \tag{2c}$$

with h equal to +1 for $\theta(t) = 0$ and -1 for $\theta(t) = \pi$. Introducing σ as the displacement of the lower level's population from its steady state value ($\sigma = \sigma_{11} - \sigma^{ss}$), and noting that $\mathrm{Im}(\dot{\sigma}_{12})$ does not interact with the other two density matrix components, results in the pertinent density matrix equations becoming

$$\dot{\sigma} = - \Gamma_1 \, (\sigma + \sigma^{ss}) + \Omega h \, \mathrm{Re}(\sigma_{12}) + 0.5 \, (\gamma_1 + B), \tag{3a}$$

$$\mathrm{Re}(\dot{\sigma}_{12}) = - \Gamma_2 \, \mathrm{Re} \, (\sigma_{12}) + 0.5 \, \Omega h \, [1-2(\sigma+\sigma^{ss})]. \tag{3b}$$

Differentiation of Eq. (3a) with respect to time, use of Eq. (3b) to replace $\mathrm{Re}(\dot{\sigma}_{12})$ in the result, and noting that $h^2 \equiv 1$ yields,

$$\ddot{\sigma} + \Gamma_1 \, \dot{\sigma} + \Omega^2 \sigma = \Omega \, \mathrm{Re}(\sigma_{12}) \, \dot{h} - \Omega h \, \Gamma_2 \, \mathrm{Re}(\sigma_{12}) + \Omega^2 (0.5 - \sigma^{ss}). \tag{4}$$

Eq. (4) has the form of a driven, damped harmonic oscillator, where the driving term is dependent on $\mathrm{Re}(\sigma_{12})$. For the moment though consider the right-hand side of Eq. (4) as a time-dependent forcing function f(t). The temporal response of σ is then given by a convolution expression,

$$\sigma(t) = \int_0^t \frac{f(t-\tau)}{\omega} \, e^{- \frac{\Gamma_1 \tau}{2}} \sin(\omega\tau) \, d\tau, \tag{5}$$

with

$$\omega \equiv (\Omega^2 - \Gamma_1^2/4)^{1/2}.$$

Treating each term on the right-hand side of Eq. (4) separately we first note that

$$\dot{h} = 2 \sum_{i=0}^{m} (-1)^i \delta(t-i\Delta t). \qquad (6)$$

$\dot{h}$ is a stream of delta-function, impulse excitations with a positive amplitude occurring whenever h changes from -1 to +1. Thus, the amplitude of the first term is instantaneously large and proportional to the value of $Re(\sigma_{12})$ at the instant of the phase change. The third term in f(t) is constant for a given set of experimental parameters. It will lead to a constant offset in σ, and from a dynamical point of view its effect may be neglected. The second term in f(t) is dependent on the full temporal evolution of $Re(\sigma_{12})$, as an initial approximation we will also neglect this term. It must be noted though that, a priori, neglecting this term lacks rigorous justifictaion, and the resulting harmonic approximation must be closely scrutinized. This approximation then only takes into account the impulsive nature of the driving term, which is associated with the system's coherence at the instant of the phase change. As we proceed with the analysis, the physical insight and limitations associated with this approximation will become more apparent.

Within the harmonic approximation the response of the system's population to a <u>single</u> phase change at t = 0 has the form,

$$\sigma(t) = \frac{2\Omega}{\omega'} \sigma^{ss}(12)\, e^{-\frac{\Gamma' t}{2}} \sin(\omega' t) \qquad t \geq 0, \qquad (7)$$

where $\sigma^{ss}(12)$ is the steady-state value of $Re(\sigma_{12})$, $\omega' = [\Omega^2 - (\Gamma_1)^2/4]^{1/2}$, and $\Gamma' = \Gamma_1$. The response is of the same general form as the experimental

response shown in Figure 2, a damped sinusoidal oscillation. Note that the amplitude of the driving term and the quantum system's response is proportional to the steady-state value of the real part of the quantum system's coherence, given by

$$\sigma^{ss}(12) = \frac{-0.25\ \Omega\hbar B}{\Gamma_1\Gamma_2 + \Omega^2} \quad . \tag{8}$$

Thus, the amplitude of population oscillations are expected to depend on the Rabi frequency in the fashion of $\sigma^{ss}(12)$. This is demonstrated in Figure 3, where the solid curve is a plot of $\sigma^{ss}(12)$ suitably normalized.

The accuracy of the harmonic approximation can be further investigated by comparing it to an analytical solution of Eqs. (2a and 2b). As the equations have constant coefficients between phase changes, Laplace transform techniques may be applied to find the dynamic behavior of σ_{11} and $\mathrm{Re}(\sigma_{12})$ in these time intervals. To include the effect of multiple phase changes, σ_{11} and $\mathrm{Re}(\sigma_{12})$ are evaluated at the instant before a phase change, and these values become the initial conditions for the Laplace transform solutions in the time interval after the phase change. While this procedure allows accurate evaluation of the density-matrix elements, it provides very little physical insight into how phase changes influence population dynamics, as all of the phase change dynamics are contained within the numerical values of the two initial conditions. Surprisingly, if $\Gamma_1 = \Gamma_2 \equiv \Gamma$ the exact population response to a single phase change is given by Eq. (7), except that now $\omega' = \Omega$ and $\Gamma' = 2\Gamma$. Comparison with the harmonic approximation shows that the oscillation frequencies are quite similiar when $\Omega > \Gamma$, but that the real oscillations decay twice as rapidly as those predicted by the harmonic approximation. Nonetheless, the comparison indicates that Eq. (7) has semi-quantitative validity, and we find it supplies physical insight into the origin of the Rabi-resonance spectrum.

In this regard we now consider the effect of a second phase change on the quantum system's population. In the harmonic approximation the driving term acquires maximum and minimum amplitudes at the oscillating coherence's

extreme values; these times are indicated as A and B in Figure 5. The effects of a second phase change at these times are displayed in Figure 7. In this figure $B/\Omega = 0.05$ and $\gamma_1 = \gamma_2 \equiv \gamma$, $\gamma/\Omega = 0.025$. The oscillation amplitudes (the exact solutions are plotted) are quite dependent on the time of application of the second phase change. At time A the magnitude of the coherence has its maximum value, resulting in an intense driving term that induces large population oscillations. The sign of the coherence and that of the delta-function produce a driving term with the same sign as that produced at the first phase change. However, the oscillations induced by the second phase change have a phase opposite to the oscillations already in progress. The new oscillations overwhelm the existing oscillations generated by the first phase change, resulting in an abrupt change in the sense of the oscillations and a cusp-like feature in the population evolution. This is shown in Figure 7(a). The enhanced oscillation amplitude is thus not due to a population resonance effect, but rather to the enhanced magnitude of the coherence-dominated driving term. At time B the signs of the delta-function and coherence again would lead to oscillations with the opposite phase of those already in progress. The coherence, though, has a small magnitude, insufficient to induce large out-of-phase oscillations, but sufficient to dampen the existing oscillations. This effect is seen in Figure 7(b).

As the temporal spacing between the two π -radian phase changes is varied, the magnitude of the first population extremum following the second phase change is correspondingly altered, producing a Rabi-resonance spectrum. In Figure 8 the theoretically generated, two-phase change, Rabi-resonance spectrum is presented ($B/\Omega = 0.05$ and $\gamma/\Omega = 0.025$). The solid line is obtained from the exact solution, whereas the dotted line comes from the harmonic approximation. As the period of time between phase changes goes to zero, the effect of the two-phase changes also disappears, and the population essentially remains in a steady state ($\sigma = 0$). The harmonic approximation provides a clear illustration of this situation. For

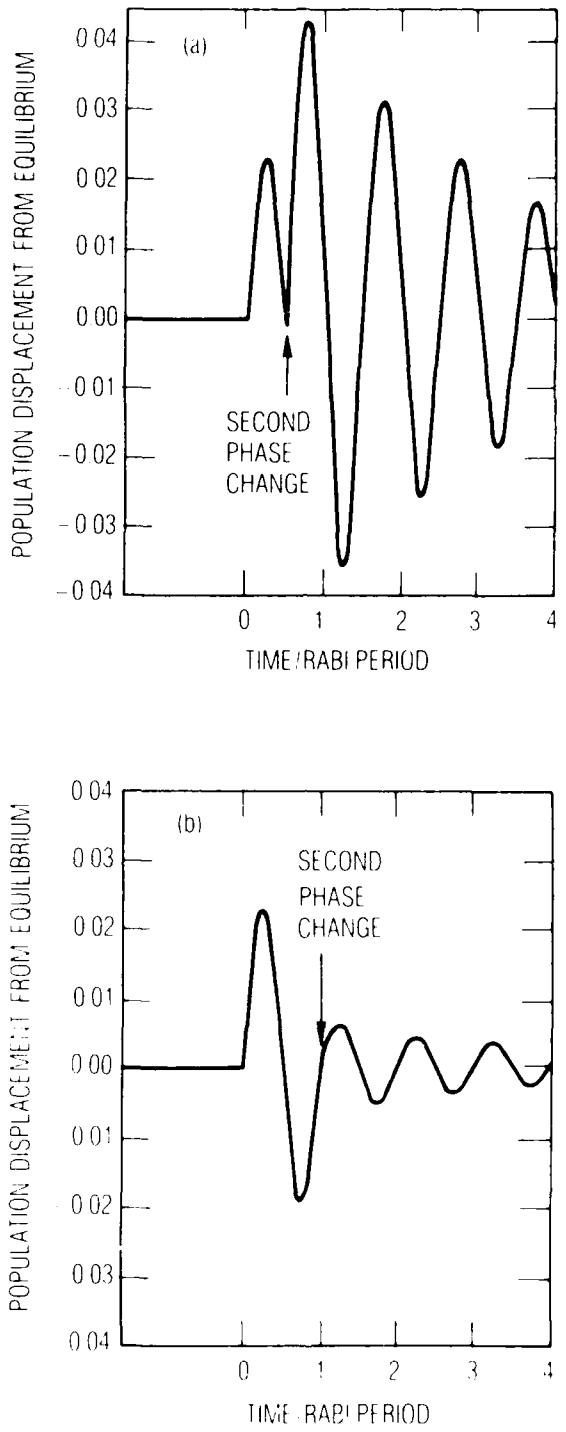

Figure 7. Population changes from equilibrium resulting from two sequential π- radian phase changes. The temporal separation between the phase changes was selected to (a) maximize and (b) minimize population oscillations after the second phase change. $B/\Omega = 0.05$ and $\gamma_1 = \gamma_2 = \gamma$, $\gamma/\Omega = 0.025$.

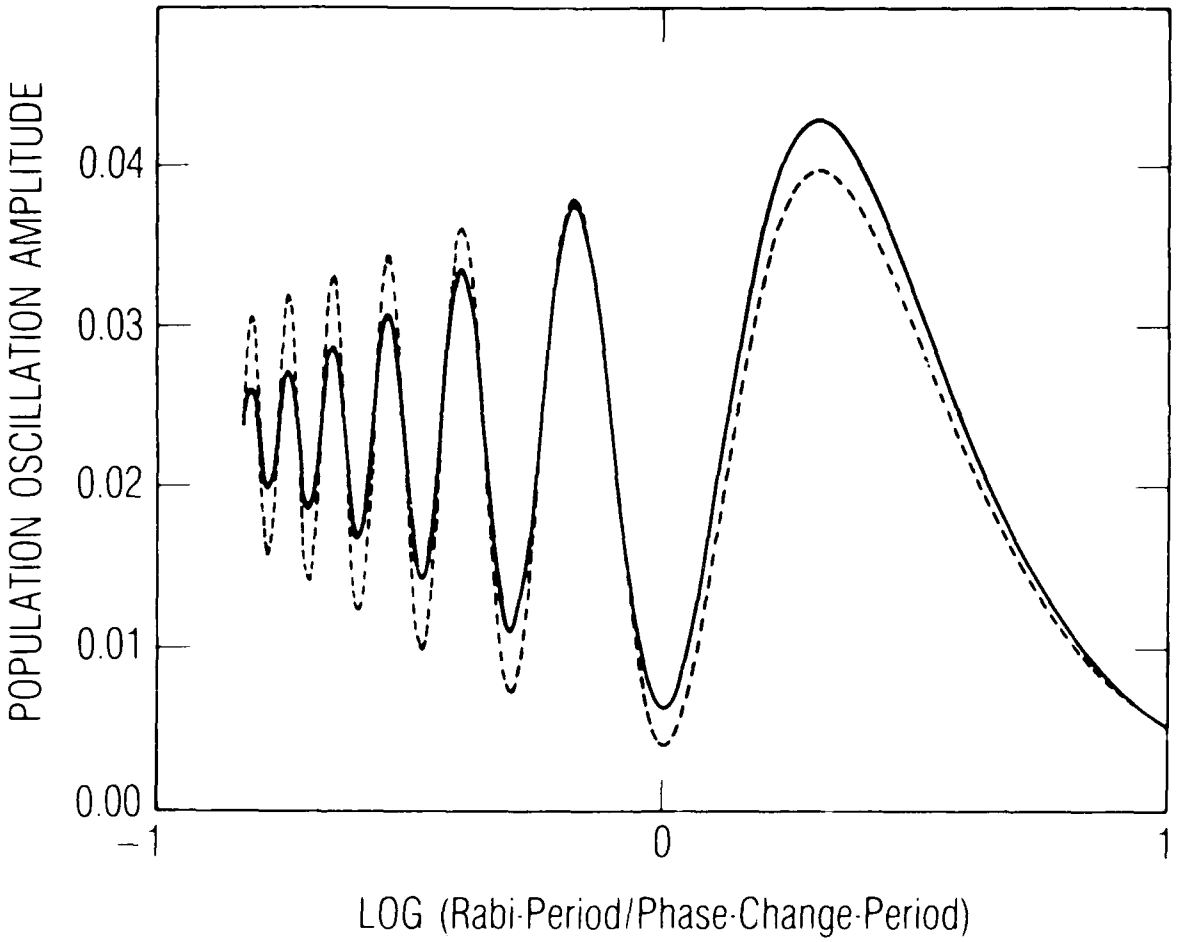

Figure 8. Comparison of the theoretical Rabi-resonance spectra resulting from the harmonic approximation (dashed line) and the exact two level density matrix solution (solid line). $B/\Omega = 0.05$ and $\gamma/\Omega = 0.025$.

sequential phase changes the delta-function contributions from $\dot{h}$ have alternating signs. If the phase changes are closely spaced in time, the system's coherence has not changed significantly between the first and second phase changes. Consequently, the atomic system is subjected to two essentially equal and opposite impulse excitations. Any population oscillation induced by the first phase change is immediately cancelled by the second. As the spacing between the two phase changes becomes large, both solutions approach asymptotically a constant value given by the quantum system's response to isolated phase changes. The harmonic approximation spectrum approaches asymptotically the isolated phase-change value more slowly than does the exact solution as a result of the differing decay rates, Γ'.

The Rabi-resonance spectrum just discussed results from <u>two</u> sequential phase changes. In our experiments, however, a continuous train of phase changes was employed, and oscillation amplitudes were extracted after the system had reached a "dynamical steady state." The theoretically generated growth of population and coherence oscillations for a sequence of phase changes, with the time between phase changes selected to maximize the growth, is shown in Figure 9. As experimentally observed [(Figure 2b)] the population oscillations display a peculiar functional form with sharp cusps at each phase change. This effect is due to the driving term, which always changes the phase of the population oscillation by 180 degrees. We also note that the coherence oscillation amplitude appears to resonantly grow with succeeding phase changes, and this in turn results in the increasing amplitude of the population oscillations.

The reason the coherence grows in the observed manner becomes apparent when Eq. (3b) is differentiated and Eq. (3a) substituted for $\dot{\sigma}$. A second harmonic equation results, and neglecting all driving terms not associated with a delta-function yields

$$\mathrm{Re}(\ddot{\sigma}_{12}) + \Gamma_2 \mathrm{Re}(\dot{\sigma}_{12}) + \Omega^2\, \mathrm{Re}(\sigma_{12}) = -\Omega\, \dot{h}\, (\sigma + \sigma^{ss} - 1/2). \qquad (9)$$

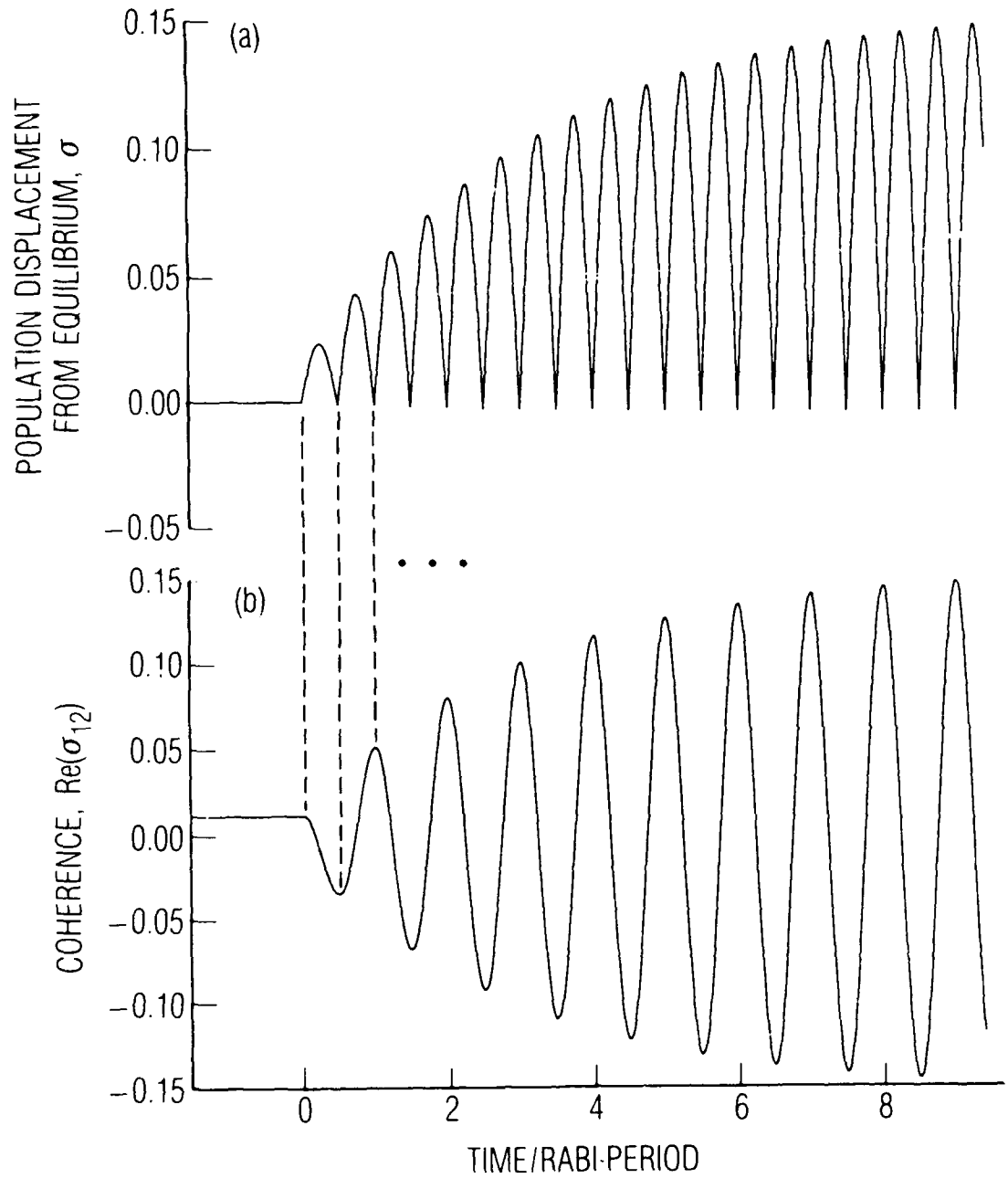

Figure 9. Theoretical population oscillations resulting from a train of π radian phase changes, with the phase changing rate selected to yield maximum population oscillations. For comparison to experiment see Figure 2b. (a) Population oscillations. (b) Coherence oscillations. $B/\Omega = 0.05$ and $\gamma/\Omega = 0.025$. The dashed lines indicate when the first few phase changes occurred.

At the instant in time when the phase changes occur, for the case of Figure 9, sigma is approximately zero, and the driving term for the coherence is simply a series of delta-functions multiplied by a single constant with alternating sign. The delta-functions occur at the extremes of the coherence oscillations with the signs appropriate to increasing the oscillation amplitude. The growth of population oscillations is driven by the coherence, and in this case the coherence oscillations are resonantly enhanced by the phase changes.

As a final, somewhat parenthetical, point we note that for very high phase-changing rates, the time-averaged value of the lower level's population asymptotically increases from its steady-state value σ^{ss} to its unsaturated value; this is in addition the amplitude of the population oscillations asymptotically approaching zero. To explain the effect we note that the adiabatic requirement on temporal variations of the electromagnetic perturbation is set by the Rabi frequency.[19,20] Consequently, for phase-changing rates much higher than the Rabi frequency, one should expect the quantum system to perform some "averaging" of the field, whereas for phase-changing rates less than the Rabi frequency, one would expect the quantum system to respond to the instantaneous values of the field. Since the average field amplitude is zero for π-radian phase changes, one would thus expect sigma approach its unsaturated value and the oscillation amplitude to asymptotically approach zero in the limit of very rapid phase changing. What is perhaps surprising, is that the harmonic approximation appears to be valid in the regime of rapid phase changing, since the theoretical Rabi-resonance spectrum shown in Figure 8 also asymptotically approaches zero. It would therefore appear that there is an initimate relationship between the proposition that the dynamical effects of sequential impulse excitations not cancel (which was discussed previously in regard to the behavior of the Rabi-resonance spectrum when the time between phase changes becomes very small) and the concept of adiabaticity.

V. SUMMARY

Expanding on the work of Cappeller and Mueller, we have investigated the Rabi-resonance phenomena (enhancements in the dynamic response of a quantum system to a train of radiation field phase changes) when the field's phase changes discretely rather than continuously. In distinction to their results, we have observed a Rabi-resonance spectrum, and have shown that the spectrum arises as a result of the discrete nature of π- radian phase changes. This spectrum is consistent with the density matrix equations describing the resonant interaction of matter with a phase changing field, and can also be understood from the perspective of a damped, driven, harmonic oscillator. In the harmonic-oscillator approximation it was shown that the enhanced population oscillations are not due to a resonance between the rate of phase changing and the population dynamics, but rather to constructively interferring impulsive force terms associated with the atomic coherence.

REFERENCES

1. A. Abragam, The Principles of Nuclear Magnetism (Oxford University, Oxford, 1961); R. G. Brewer, in Frontiers in Laser Spectroscopy, edited by R. Balian, S. Haroche, and S. Liberman (North Holland, Amsterdam, 1977), Vol. 1, pp. 341-398.

2. P. Helisto, E. Ikonen, and T. Katila, Phys. Rev. 34, 3458 (1986).

3. E. Ikonen, P. Helisto, T. Katila, and K. Riski, Phys. Rev. A 32 2298 (1985).

4. E. H. Realo, M. A. Haas, and J. J. Jogi, Sov. Phys. JETP 61, 1105 (1985).

5. E. Kh. Realo, K. K. Rebane, M. A. Khaas, and Ya. Ya. Iygi, JETP Lett. 40, 1309 (1984).

6. A. Z. Genack, K. P. Leung, and A. Schenzle, Phys. Rev. A 28, 308 (1983).

7. A. Z. Genack, D. A. Weitz, R. M. MacFarlane, R. M. Shelby, and A. Schenzle, Phys. Rev. Lett. 45, 438 (1980).

8. N. C. Wong, S. S. Kano, and R. G. Drewer, Phys. Rev. A 21, 260 (1980).

9. J. E. Golub and T. W. Mossberg, Phys. Rev. Lett. 59, 2149 (1987).

10. J. E. Golub, Y. S. Bai, and T. W. Mossberg, Phys. Rev. A 37, 119 (1988).

11. Y. L. Bai, A. G. Yodh, and T. W. Mossberg, Phys. Rev. Lett. 55, 1277 (1985).

12. U. Cappeller and H. Mueller, Ann. Phys. (Leipzig) 42, 250 (1985).

13. W. Happer, Rev. Mod. Phys. 44, 169 (1972).

14. J. C. Camparo, Contemp. Phys. 26, 443 (1985).

15. J. Vanier, Can. J. Phys. 47, 1461 (1969).

16. R. H. Dicke, Phys. Rev. 89, 472 (1953).

17. R. P. Frueholz and C. H. Volk, J. Phys. B: 18, 4055 (1985).

18. J. C. Camparo and R. P. Frueholz, Phys. Rev. A 31, 1440 (1985); Phys. Rev. A 32, 1888 (1985).

19. J. C. Camparo and R. P. Frueholz, Phys. Rev. A 30, 803 (1984).

20. J. C. Camparo and R. P. Frueholz, J. Phys. B: 17, 4169 (1984).

APPENDIX

Although the vapor may be optically thick for the temperatures employed in the present set of experiments, it can be shown that in the limit of small population oscillations (i.e., low optical pumping rates) the amplitude of the transmitted intensity oscillations is proportional to the amplitude of the population oscillations. Defining A as the amplitude of the first transmitted light intensity oscillation following the phase change, we have from Figure 2 that

$$A = I_h - I_l, \qquad (A.1)$$

where I is the level of transmitted light intensity. Now, employing the Bouger-Lambert law and taking N as the corresponding population density in the absorbing hyperfine manifold, we have that

$$A = I_o \exp(-N_h \sigma L)[1-\exp((N_h-N_l)\sigma L)], \qquad (A.2)$$

where L is the absorbing medium's length and sigma is the absorption cross-section. If $N_h \approx N_l$, then the second exponential can be expanded, and we have the final result that

$$A \sim (N_l-N_h). \qquad (A.3)$$

For the experiments described in the text, care was taken to ensure that the condition on low optical pumping rates was satisfied.

LABORATORY OPERATIONS

The Aerospace Corporation functions as an "architect-engineer" for national security projects, specializing in advanced military space systems. Providing research support, the corporation's Laboratory Operations conducts experimental and theoretical investigations that focus on the application of scientific and technical advances to such systems. Vital to the success of these investigations is the technical staff's wide-ranging expertise and its ability to stay current with new developments. This expertise is enhanced by a research program aimed at dealing with the many problems associated with rapidly evolving space systems. Contributing their capabilities to the research effort are these individual laboratories:

Aerophysics Laboratory: Launch vehicle and reentry fluid mechanics, heat transfer and flight dynamics; chemical and electric propulsion, propellant chemistry, chemical dynamics, environmental chemistry, trace detection; spacecraft structural mechanics, contamination, thermal and structural control; high temperature thermomechanics, gas kinetics and radiation; cw and pulsed chemical and excimer laser development including chemical kinetics, spectroscopy, optical resonators, beam control, atmospheric propagation, laser effects and countermeasures.

Chemistry and Physics Laboratory: Atmospheric chemical reactions, atmospheric optics, light scattering, state-specific chemical reactions and radiative signatures of missile plumes, sensor out-of-field-of-view rejection, applied laser spectroscopy, laser chemistry, laser optoelectronics, solar cell physics, battery electrochemistry, space vacuum and radiation effects on materials, lubrication and surface phenomena, thermionic emission, photosensitive materials and detectors, atomic frequency standards, and environmental chemistry.

Computer Science Laboratory: Program verification, program translation, performance-sensitive system design, distributed architectures for spaceborne computers, fault-tolerant computer systems, artificial intelligence, microelectronics applications, communication protocols, and computer security.

Electronics Research Laboratory: Microelectronics, solid-state device physics, compound semiconductors, radiation hardening; electro-optics, quantum electronics, solid-state lasers, optical propagation and communications; microwave semiconductor devices, microwave/millimeter wave measurements, diagnostics and radiometry, microwave/millimeter wave thermionic devices; atomic time and frequency standards; antennas, rf systems, electromagnetic propagation phenomena, space communication systems.

Materials Sciences Laboratory: Development of new materials: metals, alloys, ceramics, polymers and their composites, and new forms of carbon; nondestructive evaluation, component failure analysis and reliability; fracture mechanics and stress corrosion; analysis and evaluation of materials at cryogenic and elevated temperatures as well as in space and enemy-induced environments.

Space Sciences Laboratory: Magnetospheric, auroral and cosmic ray physics, wave-particle interactions, magnetospheric plasma waves; atmospheric and ionospheric physics, density and composition of the upper atmosphere, remote sensing using atmospheric radiation; solar physics, infrared astronomy, infrared signature analysis; effects of solar activity, magnetic storms and nuclear explosions on the earth's atmosphere, ionosphere and magnetosphere; effects of electromagnetic and particulate radiations on space systems; space instrumentation.